

Meter Scale Plasma Source For Plasma Wakefield Experiments

N. Vafaei-Najafabadi^a, J. L. Shaw^a, K. A. Marsh^a, C. Joshi^a, and M. J. Hogan^b

^a*Department of Electrical Engineering, University of California Los Angeles, Los Angeles, CA 90095*

^b*SLAC National Accelerator Laboratory, Menlo Park, CA 94025*

Abstract. High accelerating gradients generated by a high density electron beam moving through plasma has been used to double the energy of the SLAC electron beam [1]. During that experiment, the electron current density was high enough to generate its own plasma without significant head erosion. In the newly commissioned FACET facility at SLAC, the peak current will be lower and without pre-ionization, head erosion will be a significant challenge for the planned experiments. In this work we report on our design of a meter scale plasma source for these experiments to effectively avoid the problem of head erosion. The plasma source is based on a homogeneous metal vapor gas column that is generated in a heat pipe oven [2]. A lithium oven over 30 cm long at densities over 10^{17} cm⁻³ has been constructed and tested at UCLA. The plasma is then generated by coupling a 10 TW short pulse Ti:Sapphire laser into the gas column using an axicon lens setup. The Bessel profile of the axicon setup creates a region of high intensity that can stretch over the full length of the gas column with approximately constant diameter. In this region of high intensity, the alkali metal vapor is ionized through multi-photon ionization process. In this manner, a fully ionized meter scale plasma of uniform density can be formed. Methods for controlling the plasma diameter and length will also be discussed.

Keywords: Pre-ionized plasma, lithium, axicon, heat pipe oven, plasma wakefield accelerator.

PACS: 52.50.Jm

INTRODUCTION

A meter scale pre-ionized plasma source is needed for several beam driven plasma wakefield experiments. In electron driven experiments, such as the one at FACET, part of the SLAC National Accelerator Laboratory, the beam has to interact with self-ionized plasma in the absence of pre-ionization. In a self-ionized plasma, as the beam propagates, the ionization front moves backwards in the beam frame as the electrons at the head of the beam expand and lose the ability to further ionize. The rate of this head erosion [1] is proportional to emittance, $1/\gamma$, $1/N^{1.5}$, and $IP^{1.73}$ where γ is the relativistic Lorentz factor of the beam, N is the number of particles in the bunch, and IP is the ionization potential of the material ionized by the bunch. Head erosion is a particularly important limit in two bunch experiments which consist of a trailer beam as well as a driver bunch, where the goal is to accelerate the trailer bunch using the wake created by the driver bunch. The two bunches are created from the same initial beam since they need to fit inside a single plasma period. At FACET, this is done using a notch collimator in combination with dispersive elements [3]. The consequent reduction in the driver charge from one bunch to two bunches is 1.8×10^{10} to $6-9 \times 10^9$ which makes the head erosion problem significantly worse. Given the design parameters of FACET (see [3]) the head erosion distance in lithium and rubidium vapor sources (to be discussed in next section) will only be 20 and 30 cm respectively. In contrast, 1-2 meters of travel distance in plasma is needed to double the energy of the trailing bunch in the wake of the driver. A pre-ionized plasma would significantly reduce the head erosion of the driver, enabling the energy doubling experiment.

Proton driven experiments suffer from a similar problem. The main difficulty with high energy proton beams is that the beam density is too low for the beam to generate the plasma. The pre-ionized plasma source would enable the study of self-modulation of proton beams decoupled from ionization effects, which are of interest to experiments at SLAC and CERN [4].

The plasma source proposed in this paper will be created by laser ionization of an alkali metal vapor. The rest of the paper is thus organized: The next section describes the heat pipe oven used to create the alkali vapor targets. The ionization mechanisms considered are discussed next, and finally the ionization apparatus will be described.

ALKALI METAL HEAT PIPE OVEN

The plasma source is an ionized alkali vapor in a heat pipe oven [2]. This device, schematically shown in Figure 1, is used for its ability to create long vapor columns with uniform density profile.

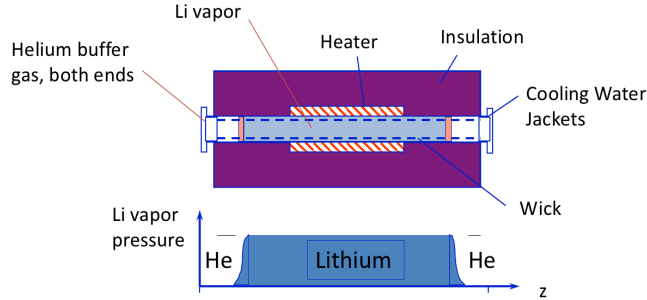


FIGURE 1. Schematics of lithium heat pipe oven (top) and the corresponding pressure (density) profile (bottom)

The operation of the heat pipe oven is as follows: The heater melts the alkali metal (e.g. lithium), creating a vapor pressure that pushes out the buffer gas (helium in the case of the lithium oven) from the central region of the oven. The vapor condenses in the helium-lithium boundary region and is then transferred back to the hot center of the oven by the wick. The water in cooling jackets on either side serves to keep the temperature of the helium low.

The pressure of the lithium vapor in the central region is equal to the pressure of the helium. This pressure in turn determines the temperature of the vapor through [5]

$$P_v(Li) = \frac{\exp(-2.0532 \ln(T) - 19.4268/T + 9.4993 + 0.753 \times T)}{133 \times 10^6} \quad (1)$$

Where T is the temperature in kilo Kelvin and P_v is the pressure in Torr. A similar equation for other alkali vapors can be found in [5]. The high thermal conductivity of the alkali vapor ensures that the temperature of the oven is uniform in the central region, which results in a uniform density. With temperature and pressure determined, the density is calculated using the ideal gas law.

Figure 2 shows experimental measurement of the temperature profile of a lithium oven (on the left) and the corresponding density profile (on the right). Since the temperature (and density) of the lithium is controlled by the pressure of helium, the heater power can be used to control the length of the oven, in case of Figure 2 creating a density profile that has a FWHM of 32 cm.

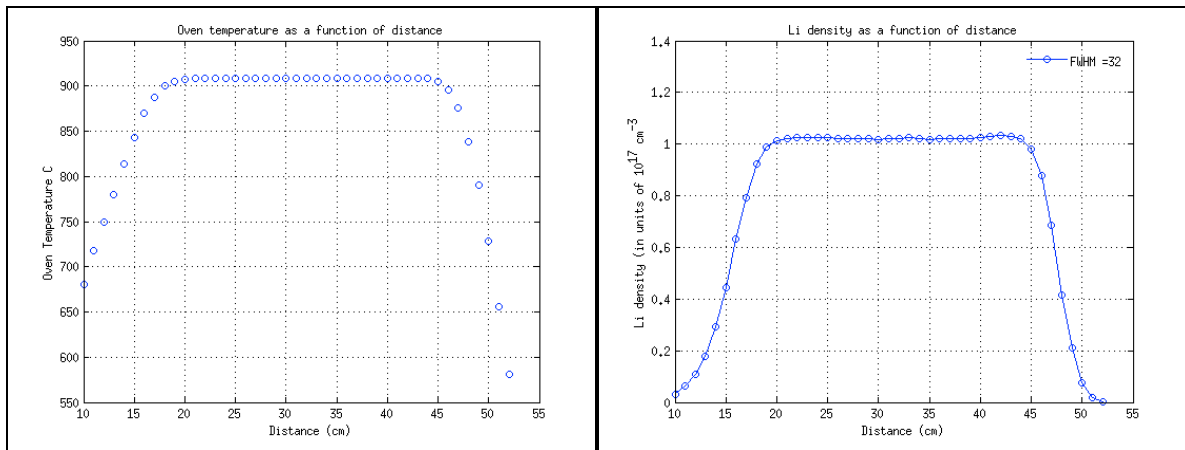


FIGURE 2. Experimental temperature (left) and density (right) profiles for a lithium heat pipe oven operating at 912 C with helium buffer pressure at 12.7 Torr, corresponding to lithium density of $1 \times 10^{17} \text{ cm}^{-3}$.

IONIZATION MECHANISM

Tunnel ionization and multiphoton ionization (MPI) are the two mechanisms that apply in the regime of laser powers of interest. In the tunnel ionization regime, the electric field of the laser modifies the potential well of the atom and the electron tunnels through the modified barrier. The equation for the tunnel ionization rate is [6]

$$W(s^{-1}) = 1.5 \times 10^{15} \frac{4^n \xi(eV)}{n\Gamma(2n)} \left[20.5 \frac{\xi^{3/2}(eV)}{E(GV/m)} \right]^{2n-1} \exp \left[-6.83 \frac{\xi^{3/2}(eV)}{E(GV/m)} \right]. \quad (2)$$

Where ξ is the ionization potential, E is the electric field, Γ is the mathematical Gamma function, and $n \approx 3.69Z/\xi^{1/2}$ is the effective principle quantum number with Z being the state of ionization; equal to one for a singly ionized atom. Equation (2) shows that the tunnel ionization rate only depends on the electric field and the ionization potential and is independent of the wavelength.

In multiphoton ionization, the photon density is so high that multiple photons are absorbed by the same atom simultaneously. The ionization rate for k photon ionization is given by

$$W(s^{-1}) = \sigma_k F^k. \quad (3)$$

Where $F=I/(h\nu)$ is the photon flux (in units of $s^{-1}cm^{-2}$) with I being the intensity of the laser and ν the frequency. σ_k (in units of $cm^{2k}s^{-k-1}$) is the multiphoton ionization cross section and depends on the material and the operating wavelength. As there is significant discrepancy in the reported theoretical values of σ_k , this parameter needs to be experimentally verified.

From the ionization rate, the electron density can be found using

$$\begin{aligned} \frac{dn}{dt} &= -Wn. \\ n &= n_0 \exp\left(-\int W dt\right) \\ n_e &= n_0 - n. \end{aligned} \quad (4)$$

Where n_0 is the initial neutral density, n is the remaining neutral density and n_e is the electron density. Ionization intensity threshold is then calculated by carrying out the integration in Equation (4) numerically over the pulse shape, seeking the intensity that results in $n_e \approx n_0$. Table (1) summarizes the ionization conditions for alkali vapors of interest (Li and Rb) along with three other gases for comparison. The multiphoton ionization threshold for lithium has been taken from the lowest of the experimental values from [7]. An 800 nm laser pulse with 50 fs FWHM has been assumed to calculate the other ionization thresholds. The three-photon cross section for rubidium is obtained from [8]. In addition to the required intensity, the energy required to ionize a satisfactory volume of gas (1 m long cylinder of 1 mm in diameter, with the density of $5 \times 10^{16} cm^{-3}$) is also stated for each element.

TABLE (1). Summary of laser ionization requirements. Tunnel ionization thresholds are calculated based on a 50 fs laser pulse. Required laser energy to generate a cold plasma of 1 mm in diameter and 1 m long, with the density of $5 \times 10^{16} cm^{-3}$

Element	IP (eV)	Ionization Threshold (Tunnel)	Energy Requirement (mJ)	Ionization Threshold (MPI)
Rb	4.17	$2.6 \times 10^{12} Wcm^{-2}$	26	$4.2 \times 10^{11} Wcm^{-2}$
Li	5.39	$7 \times 10^{12} Wcm^{-2}$	34	$4 \times 10^{11} Wcm^{-2}$
H ₂	13.6	$1 \times 10^{14} Wcm^{-2}$	85	--
Ar	15.6	$1.5 \times 10^{14} Wcm^{-2}$	98	--
He	24.6	$1.4 \times 10^{15} Wcm^{-2}$	155	--

As the table shows, the dominant process for ionization of alkali vapors with $IP < 6$ eV is the multiphoton ionization with a threshold that is at least 5 times less than the tunnel ionization threshold. In contrast, the dominant ionization process for hydrogen, helium, and argon is tunnel ionization. In general, the tunnel ionization has higher

threshold and creates higher temperature plasmas with lower recombination rate compared to MPI. However, recombination happens on a time scale of over 1 ns and the delay between laser and electron beam can be set within a 100 fs. Therefore the effect of recombination is not a concern.

IONIZATION APPARATUS

Lens

The initial idea of using a long focal length lens to ionize the vapor sources in the heat pipe oven was eventually abandoned due to

1. Concern about the nonlinear effects in alkali vapors and the possibility of filamentation.
2. Concern about the large energy volume in the Gaussian focusing geometry, while only a portion of it will be useful. The usable width of the generated plasma is limited to the smallest ionization diameter, which is at the focus.
3. The laser mode has to be a perfect Gaussian for the ionization contour calculation to be reliable. Unfortunately this is very difficult to achieve with high power lasers.
4. Since the path of the particle beam needs to be clear, the laser would have to be coupled to the vapor source using a holed mirror. However, this results in a hollow transverse laser profile in the focal region, which translates to a hollow plasma, contrary to our goal of constructing a uniform plasma.

Axicon

An axicon is an optical element with conical cross section. As shown in Figure 3, this shape gives the axicon the ability to bend all the incoming rays by the same angle. This results in a region of interference which is called the focal region of the axicon. Using the Kirchhoff diffraction integral, for the region near the optical axis, the intensity profile can be calculated as [9]

$$I(r, z) = \frac{\pi k \sin(\gamma)}{2} \frac{z}{C_\alpha} I_{in}(\rho(z)) \left[\frac{1 + \cos \gamma}{2} J_0(kr \sin \gamma) + \frac{1 - \cos \gamma}{2} J_2(kr \sin \gamma) \right]^2 \quad (5)$$

The intensity on axis is then given by

$$I(z) = \frac{\pi k \sin(\gamma)}{2} \frac{z}{C_\alpha} I_{in}(\rho(z)) \frac{(1 + \cos \gamma)^2}{4} \quad (6)$$

Where

$$z(\rho) = \rho C_\alpha = \rho \left[\frac{1}{\tan \gamma} - \tan \alpha \right] \quad (7)$$

Equation (7) gives the explicit mapping of the radius ρ , where a ray intercepts the axicon, to the longitudinal location z , where this same ray crosses the optical axis. In these equations, k is the wave number, α is the axicon angle, γ is the angle of approach given by $n \times \sin \alpha = \sin(\alpha + \gamma)$ where n is the index of refraction, and J_0 and J_2 are Bessel functions of the first kind of zero order and second order respectively.

Using Equation (6), the longitudinal on-axis profile for an 8 TW 800 nm laser pulse is plotted in Figure 4(a) for a plane wave (green curve) and for a Gaussian intensity profile with 2 cm FWHM (blue curve). These plots are made for an axicon of two inch diameter with $\alpha=1$ degree. As it appears from Table (1), the on axis intensity exceeds even the ionization threshold of argon for over 1.5 meters. However, the transverse profile of the axicon is strongly

affected by the Bessel terms in Equation (5), as can be seen from Figure 4(b). If we used argon, we would have a very narrow plasma column indeed. With the alkali metal vapors on the other hand, each of the Bessel peaks will separately ionize the gas and with the MPI ionization threshold being as low as $4 \times 10^{11} \text{ Wcm}^{-2}$, it is likely that the region of ionization will be uninterrupted and as wide as several hundred microns.

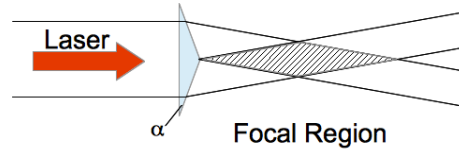


FIGURE 3. Schematics of axicon

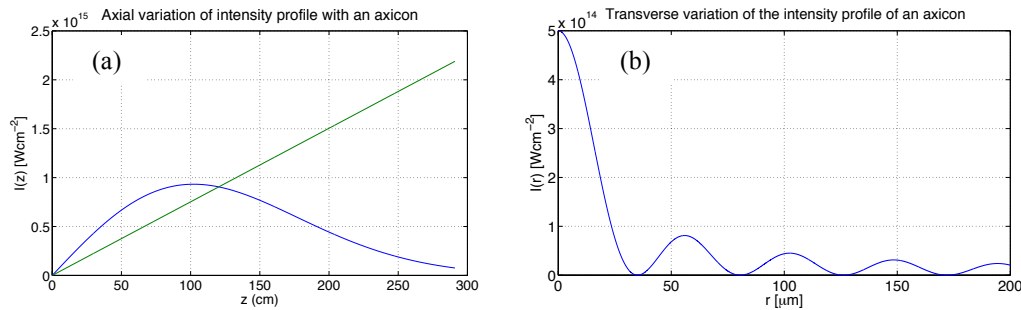


FIGURE 4. (a) Axial variation of intensity for an 8 TW, 800 nm laser pulse for a plane (green) and Gaussian profile of 2 cm FWHM (blue). (b) Transverse intensity profile adjusted to the peak intensity of $5 \times 10^{14} \text{ Wcm}^{-2}$

The images in Figure 5 demonstrate plasma emissions observed from hydrogen, argon, and helium when irradiated with a Ti:Sapphire laser pulse with less than 3 TW of power using an axicon one inch in diameter with $\alpha=0.5$ degree. Because of the large difference between the ionization threshold of helium and the other gases (see Table (1)), plasma emission from helium implies the full ionization of hydrogen and argon. The emission observed is about 100 microns wide and is longer than the field of view of camera in Figure 5 We have separately measured emission lengths as long as 40 cm long using only 700 GW of laser power and a two degrees axicon. With a higher power laser, a larger diameter axicon with smaller angle, and using alkali metal vapors we can generate longer and wider plasma columns.

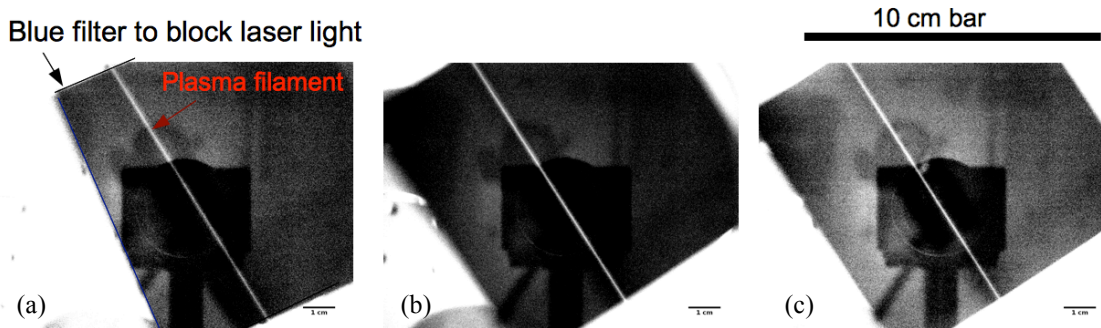


FIGURE 5. Emission observed by a camera looking into the vacuum chamber filled with the hydrogen (a), argon (b), and helium (c). Laser power on the axicon was 2.2 TW, 1.8 TW, and 2.9 TW for (a), (b), and (c) respectively. A one inch wide, 0.5 degree axicon was used to ionize the gases. A blue filter was used to block the light from the laser. The reflection of the camera looking at the blue filter is seen in the pictures as well.

Furthermore, it is possible to change the spot size diameter of the Bessel beam by controlling the incoming laser phase front. In the preliminary experiments using a single lens before the axicon, the peak-to-zero of the Bessel spot increased from about 80 microns to 700 microns by adjusting the distance between the lens and the axicon (See Figure 6). There is however a tradeoff between the size of the central spot and its intensity.

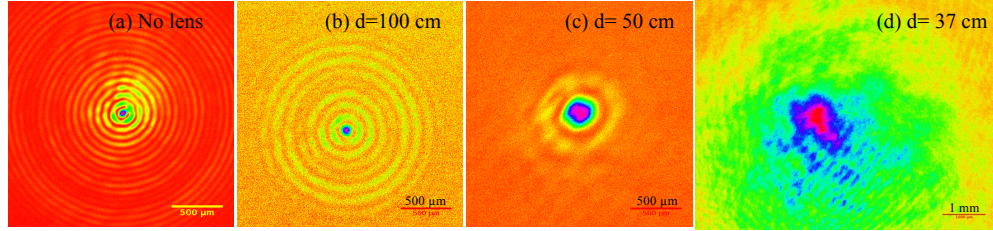


FIGURE 6. Variation of Bessel spot in the presence of a lens before the axicon. A 26 cm focal length lens is used at distance ‘d’ upstream of the one inch diameter $\alpha=0.5$ degrees axicon, with the observation plane 50 cm downstream of the axicon. The first zero of the Bessel function is 70 μm , 80 μm , 250 μm , 700 μm for (a),(b), (c), and (d) respectively.

Finally, as previously mentioned, because the path of the particle beam needs to be clear, the laser has to be coupled to the vapor source using a holed mirror. This requirement can easily be satisfied with an axicon because the rays that intercept the optical axis at different locations come from different radii on the axicon. So blocking the center rays will not affect the ones that merge later on. This was experimentally verified by blocking 3.5 mm of the center of the axicon with the result that the intensity of the central spot recovered after about 60 cm.

SUMMARY

To avoid the head erosion problem, we plan to use a short pulse Ti:Sapphire laser in combination with an axicon to ionize lithium vapor. We have demonstrated 40 cm long ionized gas column using sub-TW short pulse Ti:Sapphire laser to overcome ionization threshold of over 10^{14} Wcm^{-2} . The emission diameter of the column was about 100 microns. The plasma length and diameter can be controlled by the laser beam parameters. This can be done using telescopes, apertures, phase masks, and axicon selection. Longitudinal modulations in the axicon intensity and plasma profiles should be corrected, but this is not a concern if the plasma can be fully ionized. Larger diameter plasmas can be produced in metal vapors because of the reduced ionization threshold requirement and a relatively large number of axicon peaks capable of ionizing.

ACKNOWLEDGMENTS

The authors gratefully acknowledge support by DOE (grant DE-FG02-92ER40727) and NSF (grant PHY-0936266). This work was support with government support under and awarded by DoD, Air Force Office of Scientific Research, National Defense Science and Engineering Graduate (NDSEG) Fellowship, 32 CFR 168a (Shaw), and NSERC Canada PGS-D (Vafaei);

REFERENCES

1. I. Blumenfeld et al., *Nature* **445**, 741-744 (2007).
2. P. Muggli et al., *IEEE Transactions on Plasma Science* **27**, 791-799, (1999).
3. M. J. Hogan et al., *New Journal of Physics* **12**, 055030 (2010).
4. G. Xia et al., *Journal of Plasma Physics*, pp. 1-7 (2012).
5. A. G. Mozgovoi et al., *High Temperatures. High Pressures* **19**, 425-430 (1987).
6. D. L. Bruhwiler et al., *Physics of Plasmas* **10**, 2022 (2003).
7. M. Schuricke et al., *Physical Review A* **83**, 1-11 (2011).
8. E. McGuire, *Physical Review A* **23**, 186-200 (1981).
9. C. G. Durfee III, J. Lynch, H. M. Milchberg, *Physical Review E* **51**, 2368 (1995).